SUPPLEMENTAL INFORMATION

GRK2 regulates physiological and tumoural vascularization

Verónica Rivas [1,2], Rita Carmona [3], Ramón Muñoz-Chápuli[3], Marta Mendiola [4], Laura Nogués [1,2], Clara Reglero [1,2], María Miguel-Martín[4], Ramón García-Escudero [5], Gerald W Dorn II [6], David Hardisson [4,7], Federico Mayor, jr. [1,2,*] and Petronila Penela[1,2,*]

[1] Departamento de Biología Molecular and Centro de Biología Molecular "Severo Ochoa", Universidad Autónoma de Madrid, 28049 Madrid, Spain,

[2] Instituto de Investigación Sanitaria La Princesa, 28006 Madrid, Spain

[3] Department of Animal Biology, University of Málaga, Málaga, Spain

[4] Laboratory of Pathology and Oncology, Research Unit, Hospital Universitario La Paz, IdiPAZ, Madrid, Spain

[5] Molecular Oncology Unit, Division of Biomedicine, CIEMAT, Madrid, Spain

[6] Washington University Center for Pharmacogenomics, St. Louis, MO 63110, USA

[7] Department of Pathology, Hospital Universitario La Paz, School of Medicine, Universidad Autonoma de Madrid, IdiPaz, Madrid, Spain

SUPPLEMENTAL FIGURE LEGENDS

Figure S1. Effect of GRK2 protein reduction on the proliferative and chemotactic responses of primary endothelial and vascular smooth muscle cells. (A) Neither ERK1/2 nor AKT signalling in response to 20 ng/ml VEGF is affected in MLECs by the expression levels of GRK2. VEGF induced-activation of ERK1/2 and AKT was determined in MLEC isolated from wild-type or GRK2 hemizygous mice by immunoblotting using specific antibodies as described in Methods. Phospho-protein

band densities were normalized to cognate total protein values. Data are mean±SEM from 3-4 independent experiments. (B) GRK2 protein levels do not influence the proliferation of angiogenic factors-stimulated endothelial cells. Proliferative capacity of MLEC-GRK2+/+ and GRK2+/- cells was analyzed in response to 1μM S1P, 20 ng/ml VEGF or 5% serum (FCS) by using a H3-thymidine uptake assay as described in Methods. Data are mean± SEM of 3 independent experiments. (C,D) Decreased GRK2 expression enhances motility of vascular cells in response to angiogenic factors. Serum-starved MLEC (C) or aortic vascular smooth muscle (D) cells derived from GRK2+/+ or GRK2+/- mice were subjected to migration assays towards 50 ng/ml PDFG-BB or 20 ng/ml VEGF, respectively, as detailed in Methods. Data are mean±SEM of 2-4 independent experiments performed in duplicate. P values are indicated.

Figure S2. Endothelial-specific GRK2 downregulation impedes proper in vivo and in vitro formation of vessel-like structures in response to angiogenic stimuli. (A-C) In vivo vessel formation is compromised in mice expressing different levels of vascular GRK2. Global hemizygous GRK2 mice (A), endothelial-specific heterozygous Tie2Cre-GRK2 f/+ animals (B) and hemizygous mice (Tie2Cre-GRK2 f/-) with an extra reduction of GRK2 specifically at endothelium (C) display severe defects in the vessel-like organization of both endothelial and mural cells in response to angiogenic stimuli. Sections of S1P (A) or FGF2 (B, C)-embedded Matrigel plugs excised from these animals were analyzed by immunohistochemistry with anti-mouse CD31 and NG2 antibodies and DAPI staining as indicated. (D) Comparative analysis of GRK2 expression in endothelial and non-endothelial cell populations of wild-type, global hemizygous (GRK2+/-) or GRK2+/-;Tie2-Cre-GRK2 f/- mice. Fibroblasts, macrophages and endothelial cells were obtained from the lungs of the different mice. Pulmonary mixed-cell populations were first subjected to a sorting step that selects

macrophages (negative selection), and the remaining cells were then sorted to separate MELCs (positive selection) from fibroblasts as detailed in Methods. Levels of GRK2 were analyzed in whole cellular lysates by immunoblotting with a specific anti-GRK2 antibody (Ab C-15). Actin and GAPDH expression were used as loading controls and fold-expression of GRK2 normalized to loading is included above each blot. Gels are representative of 2 independent experiments. (E) Effect of vascular GRK2 downmodulation in the endothelial expression of other GRK family members. Levels of GRK3 and GRK6 were determined in cell lysates of MLEC isolated from wt mice or GRK2 hemizygous mice by using the polyclonal anti-GRK2 antibody FP1, which also recognizes GRK3, and a specific anti-GRK6 antibody (Ab C-20). Non-contiguous lanes run in the same gel are indicated by a black vertical line. (F) GRK2 down-regulation attenuates the stimulatory effect of FGF2 in the tube formation response of endothelial cells. MLECs from wild-type (GRK2+/+) or global hemizygous (GRK2+/-) GRK2 mice were seeded on Matrigel-coated wells in the presence of 50 ng/ml FGF2. Photographs were taken after 16-18h in culture (x5 magnification) and tube formation network was quantified using the online software of Wimasis. Tube formation index (mean±SEM) was defined as described in Methods. Each condition was assayed 2 times in duplicate. P values are detailed. Scale bar, 500μm (panel F), 100μm (panel B, C) and 50 μm (panel A) .

Figure S3. Altered TFGβ1 signaling, secretion profile and impaired barrier function in endothelial cells with deficient GRK2 expression. (A) ECs with reduced expression of GRK2 are more sensitive to dose-dependent inhibitory effects of TGFβ1 on cellular proliferation. Proliferation of EC induced by 1μM S1P was analyzed in the presence of TGFβ1 at the concentrations indicated. Data are mean± SEM of 4 independent experiments. (B, C) GRK2 downmodulation differentially modulates

TGFβ1 signaling mediated by ALK1 and ALK5 receptors in endothelial cells. Stimulation of Smad2/3 (B) and Smad1/5/8 signaling branches (C) in response to 5ng/ml TGFβ1 was determined in serum-starved MLEC-GRK2+/+ or –GRK2+/- cells that were previously pre-incubated or not with either 5μM A8301 or 3μM SIS3 in order to block ALK5 or Smad3 activation, respectively. (B) In GRK2+/- cells, the relief of the inhibitory GRK2-mediated phosphorylation of Smad2/3 (that prevents its activation by ALK5) underpins increased activation of the Smad2/3 branch by TGFβ1. Inhibition of ALK5 blunts TGFβ1-induced stimulation of Smad2/3 in both wt and GRK2+/- cells, but exogenous inhibition of Smad3 by SIS3 is less efficient in GRK2+/- cells. Higher levels of inhibitory phosphorylation of Smad3 by GRK2 in wt cells would synergize with the mechanism of action of SIS3, resulting in greater ratios of inhibition. (C) Differential activation of Smad1/5/8 in wt and GRK2+/- cells is not sensitive to SIS3-dependent inhibition of Smad3, suggesting that a negative crosstalk from ALK5 to ALK1 signaling at the level of Smads is not involved and pointing to an intrinsic effect of GRK2 in the ALK1-Smad1/5/8 branch of signaling. Conversely, GRK2 reduction can alleviate the reported lateral inhibition of ALK1 on ALK5-Smad2/3 signaling, leading to increased activation of Smad2/3. (D) Cell culture-supernatants of serum-starved MLEC-GRK2+/+ and –GRK2+/- cells maintained in quiescence for 48h were processed for detection of different angiogenic modulators by using an specific mouse angiogenesis antibody array as detailed in Methods. Spots were analyzed by laser densitometry and data (mean±SEM) from three independent experiments were graphically expressed as fold-change of factor secretion in MLEC-GRK2+/- cells compared to that in control cells. GRK2 downregulation correlates with decreased secretion of anti-angiogenic cytokine and angiostatic factors such as trombospondin-1 (TSP1) (Bornstein, 2009), IL13 (Kiefer and Siekmann, 2011) or PF-4 and IP-10 (Belperio et al, 2000).. Production of factors

that contribute to endothelial tube formation such as IL6, IL1α or TNFα is also impaired in MLEC-GRK2+/- cells. (E) Permeability of endothelial cell monolayers from wild-type and GRK2 hemizygous mice in the presence or absence of VEGF. Primary MLEC-GRK2+/+ and GRK2+/- cells were grown in transwell inserts for several days to reach confluence and then stimulated with 20 ng/ml VEGF or vehicle. Vascular permeability to HRP was assessed by a colorimetric method as indicated in Methods. GRK2+/- endothelial cells display increased permeability in both basal and VEGF-stimulated conditions. Data are mean±SEM from two independent experiments. P values are indicated.

Figure S4. Vascular loops, pericyte coating and vascular pruning during retinal development are impaired in mice with specific endothelial downregulation of GRK2. (A-B) Quantification of vascular loops and the degree of pericyte expansion on vascularized P9 retinas. Whole-mount retinas from wt (GRK2 f/f) and Tie2Cre-GRK2-f/f mice were stained with the endothelial marker ILB4-FITC (A) or with a specific anti-NG2 antibody (B). (A) Loops of the capillary network were manually counted by two investigators in a blinded fashion in low-magnification fields (n= 11 in retinas of 4 GRK2 f/f mice and n= 12 in retinas of 5 Tie2Cre-GRK2f/f animals). The ratio of total loops per vascular area (μm) was represented. Scale bar, 100μm. (B) The ratio between the NG2-positive area and total field area of the retina was plotted (n=15 images from retinas of 5 GRK2 f/f wild-type mice=5 and n=12 from retinas of 5 Tie2Cre-GRK2 f/f. mutant animals). (C, D) There was a defective pruning of retinal vasculature by P14 in Tie2Cre-GRK2 f/f mice compared to wt animals, despite bearing a similar extent of pericyte coverage. Whole-mount P14 retinas were double-stained with ILB4-FITC and anti-NG2 antibodies and the corresponding positive areas were quantified as detailed in Methods. (C) A significant increase in both branching of primary vascular plexus and

vascular endothelial and pericyte densities was observed in P14 Tie2Cre-GRK2 f/f retinas. For branching quantification, images (10x magnification) of GRK2 f/f (n=9; mice=5) and of Tie2Cre-GRK2 f/f (n=8; mice=5) were analyzed. For vascular densities, 10x amplification fields were quantified (n=11; GRK2f/f mice=5 and n=8; Tie2Cre-GRK2 f/f mice=5). Scale bars, 132μm. (D) By P14, pericyte covering of retinal vessels in Tie2Cre-GRK2 f/f pups equals those of wt animals. Coverage was expressed as the percentage fraction (mean±SEM) of co-localizing pericyte- and endothelial-positive areas in high magnification fields (n=12; GRK2 f/f mice n=5 and n=20; Tie2Cre-GRK2 f/f mice=5). P values are included.

Figure S5. Additional features of the vascular phenotype of systemic GRK2 knockout embryos at the E10.5 stage. (A-D) Lack of vascularization in the hindbrain (hb) of GRK2-/- embryos (C, D) as compared with the wildtype (A,B). PECAM1-positive vessels can be seen within the neural tissue on the wildtype embryos (arrows). The perineural vessels (pn) on the mutant appear abnormally dilated. Fb: forebrain. (E-H) Abnormal mural cell coverage in the paired aortas (ao) of GRK2-/- embryos (F,H) as compared with the wildtype (E,G), as demonstrated by SMA immunostaining. The posterior left aorta shows a much reduced diameter (arrow in H). Aortic endothelium shows discontinuities (arrow in J) in the knockout animals. Abnormal dilatation of the vessels is also observed in the limb bud of the GRK2-/- embryo (arrow in L). Scale bars, 50μm, except 25μm in A and B.

Figure S6. Lack of GRK2 expression results in vascular haemorrhages and mesenchymal apoptosis. (A) Expression pattern of GRK2 in large embryonic vessels. Histological sections of E10.5 wild-type embryos were labelled with the polyclonal anti-GRK2 antibodies C-15 or FP2, that recognize different regions of GRK2 in the C-terminal half of the protein. Both antibodies reveal similar patterns of vascular GRK2

staining. The endothelium of the dorsal aorta and cardinal vein is clearly labelled with the C-15 antibody (arrows). Some perivascular cells of the mesenchyma are also positive for GRK2 expression (arrowheads). ao: aorta, cv: cardinal vein, dc: duct of Cuvier. Sections of the dorsal aorta were stained with anti-SMA (red) and anti-GRK2 FP2 (green) antibodies. Co-localization of GRK2 with SMA signals indicates the presence of GRK2 in cells throughout the aortic media, confirming the pattern obtained with the anti-GRK2 antibody C-15 (Figure 5). Scale bar, 50µm. (B) Eosin-hematoxylin-stained sections of E10.5 GRK2 knockout embryos shown defective organization and integrity of the aortic wall (arrow) with hemorrhagic blood cell accumulation (arrowhead). Scale bar, 25µm (left) 50µm (middle) 100µm (right). (C) GRK2 expression was analyzed in whole body homogenates of wt, GRK2 +/- and GRK2 -/- mice. Non-contiguous lanes run in the same gel are indicated by a black vertical line. Ponceau-blot staining and a non-specific protein band serve as controls of protein loading (D) Activated-caspase-3 immunostaining of E10.5 GRK2-null embryos showing extensive areas of mesenchymal apoptosis. Scale bar, 100µm.

Figure S7. **Reduced expression of endothelial GRK2 alters the functionality of tumor-induced in vivo angiogenesis and secretion of macrophage pro-recruiting factors.** (A) Tumor-driven neovessels in mice deficient for GRK2 expression show impaired blood vessel perfusion compared to those in wild-type mice. Matrigel (0.5ml) was mixed with B16F10 melanoma cells ($1x10^6$) or vehicle and then injected into wild-type (GRK2+/+) or global hemizygous (GRK2+/-) mice. Hemoglobin quantification was performed on plugs removed after 7 days with the TMB liquid substrate system as described in Methods. Data are mean±SEM from 9 animals for each condition in 3 independent experiments. (B, C) Increased endothelial production and secretion of factors related to macrophage mobilization and extra-vascular infiltration in response to

GRK2 downregulation. Cell culture-supernatants of serum-starved MLEC-GRK2+/+ or GRK2+/- cells maintained in quiescence for 48h were processed for detection of CXCL12 (B) and other different factors (C) by using an specific mouse angiogenesis antibody array as detailed in Methods. Reduced endothelial expression of GRK2 results in higher levels of several potent macrophage chemoattractants such as GM-CSF, PIGF2 (Adini et al., 2002), Factor III (Gil-Bernabe et al., 2012) or CXCL16 (Zhang et al., 2009). Production of factors that contribute to facilitate monocyte adhesion to and diapedesis through endothelial layers such as CXCL12 and ET-1 (Dirkx et al., 2006) is also increased in MLEC-GRK2 +/- cells. In addition, secretion of the KC cytokine, involved in monocyte chemotaxis (Traves et al., 2004) and monocyte arrest on the endothelium from flow and diapedesis (Smith et al, 2005) is strongly upregulated in the conditioned media of these cells. Moreover, MLEC-GRK2 +/- cells produce lower levels of VEGF isoforms, which reduced local endothelial exposure has been reported to facilitate monocyte infiltration because these pro-angiogenic factors downmodulate endothelial adhesion molecules involved in monocyte tethering and rolling (Dirkx et al., 2006). P values are included. ns, not significant

Figure S8. Expression of GRK2 in the endothelium is regulated in normal and pathological conditions at the transcriptional level. (A) The GRK2 mRNA levels in endothelial cells are increased in physiological contexts of angiogenesis. Tags from regenerating liver (RL) were compared to the total tags derived from the normal endothelial liver library. The top 13 TEM genes with the highest tag ratios in regenerating ECs compared to all non-regenerating endothelial libraries are shown. Tag numbers for each group were normalized to 100,000 transcripts. (B) Endothelial mRNA levels of GRK2 are downregulated by tumor cells. HMVECs co-cultured with LS180 tumor cells in the presence of blood components displayed under-expression of

the GRK2 transcript. mRNA expression values of GRK2 are shown as mean values ± SD (log2 scale) of biological triplicates from genome-wide microarray analysis (see Methods). Significant differences in expression levels were tested using Student's T test. ns, not significant

SUPPLEMENTAL METHODS

Reagents and Antibodies.

Affinity-purified rabbit polyclonal antibodies raised against GRK2 (C-15), GRK6 (C-20), the affinity-purified goat polyclonal antibody raised against actin (I-19), the affinity-purified rabbit polyclonal antibody anti-Smad1/5/8 (N-18), and the polyclonal C-16 and C-14 antibodies that recognize ERK1 and ERK2, respectively, were purchased from Santa Cruz Biotechnology.The rabbit polyclonal antibodies raised against anti-phospho-ERK1/2, anti-phospho-Smad2, anti-phospho-Smad1/Smad5/Smad8, anti-Smad2/3, anti-pSer473-AKT and anti-AKT were purchased from Cell Signaling Technologies. A GAPDH mouse monoclonal antibody (6C5) was from Abcam. The polyclonal antibody Ab-FP2, raised against a GST fusion protein including the C-terminal region of GRK2 has been previously described (Salcedo et al., 2006). Biotinylated *Griffonia (Bandeiraea) simplicifolia* Lectin I Isolectin B4 was obtained from Vector Laboratories. Rabbit polyclonal anti-adrenomedullin antibody was supplied by Novus Biologicals. Rat monoclonal anti-CD31 (PECAM-1), rat anti-mouse FCγRII/III and rat anti-ICAM2 were from BD Pharmingen TM. Rabbit polyclonal antibody anti-NG2 was from Millipore. Rabbit anti-caspase 3 (activated) polyclonal antibody was purchased from Promega. Magnetic beads (Dynabeads) coated with sheep anti-rat antibody were obtained from Dynal.

The PI3K inhibitor LY 294002 and PDGF-BB were purchased from Calbiochem, the specific Smad3 inhibitor SIS3 was from SIGMA, and the ALK5 inhibitor A83-01 was from Santa Cruz Biotechnology. Heparin, fibronectin (FN), sphingosine 1-phosphate (S1P), 3,3′,5,5′-tetramethylbenzidine liquid substrate system (TMB) and Horseradish Peroxidase (HRP) were obtained from SIGMA. Vitrogen 100 was from Cohesion and endothelial cell growth supplement (ECGS) from AbD Serotec. Matrigel basement

membrane was purchased from BD Biosciences. Collagenase type I and the ligands TGFβ1 and BMP9 were from Gibco and R&D systems, respectively. VEGF, recombinant murine IL-4 and FGF2 were obtained from Peprotech. Avidin-biotin-peroxidase complex (Elite ABC kit) and diaminobenzidine (DAB) were purchased form Vector Laboratories. All other reagents were of the highest commercially-available grades.

Animals and Genotyping

Systemic GRK2 gene disruption is lethal at early gestational age (Jaber et al., 1996), but hemizygous GRK2 mice (GRK2+/-) are viable and apparently normal. Genotyping of these mice was performed as previously described (Penela et al., 2008). Floxed GRK2 mice were generated with loxP sites flanking exons 3–6 as reported (Matkovich et al., 2006). Endothelium-specific GRK2 knock-out mice (Tie2Cre-GRK2 f/f) were generated by mating GRK2-floxed mice and transgenic endothelial Tie2-Cre animals, in which expression of Cre recombinase is driven by the endothelial-specific promoter of the Tek (Tie2) receptor. These conditional knock-out mice and control non-transgenic floxed GRK2 mice were transferred from Dr. Walter J. Koch laboratory (Temple University, Philadelphia, USA). The Tie2Cre-GRK2 f/f mice were identified by genotyping tail cDNA by PCR using primers that specifically recognize floxed GRK2 alleles [oligos A (5'-CAGGCATTCCTGCTGGACTAG-3') and B (5'-TGAGGCTCAGGGATACCTGTCAT-3')] and recombined (deleted) GRK2 alleles [oligos A and C (5'-GTTAGCTCAGGCCAACAAGCC-3')] as described (Matkovich et al.,2006). Presence of Cre-recombinase was evaluated by PCR according to the protocol provided by The Jackson Laboratories (JAX mice database). Some inter-individual variability of allele recombination was noted despite homogenous genetic background of littermates, as inferred by the different ratio of the floxed vs deleted

allele-amplified products, what suggests that Cre-lox technology is not 100% effective and that potential intra-individual chimerism might occur (Matkovich et al., 2006). We also generated "hybrid" animal models in which individuals express different extra-endothelial GRK2 protein levels in combination with distinct endothelial GRK2 content by crossbreeding systemic hemizygous GRK2 (GRK2+/-) with homozygous Tie2-CreGRK2 f/f mice. As a result, approximately 50% of the offspring displayed wildtype systemic GRK2 levels with endothelial GRK2 f/+ heterozygosity, while the remaining 50% was systemic hemizygous for GRK2 with endothelial GRK2 f/- hemizygosity.

Cell Culture, Co-culture Assays and Cellular Sorting.

Primary mouse lung endothelial cells (MLEC) were obtained from mice expressing different dosages of systemic (GRK2 +/+, GRK2 +/-) and/or endothelial GRK2 expression (Tie2Cre-GRK2 f/+, Tie2Cre-GRK2 f/- and Tie2Cre-GRK2 f/f) by using a digestion and magnetic-bead cell sorting method (Reynolds et al., 2002).Briefly, mouse lungs were minced, collagenase-digested and further disaggregated to obtain a single cell suspension. Endothelial cells were isolated from this mixed-cell population by means of a single negative selection step with anti-mouse FCγ-RII/III monoclonal antibody followed by positive selection with anti-mouse ICAM-2 mAb and anti-IgG-coated magnetic beads. The endothelial population was >90% pure as assessed by anti-mouse CD31 staining. MLECs were plated on dishes coated with a mix of 0.1% gelatin, 10 mg/ml fibronectin and 30 µg/ml Vitrogen 100, and grown in the presence of DMEM plus Ham's F-12 (1:1) containing 20% FBS, 100µg/mL heparin and ECGS (ABD, Serotec). The cells were propagated in 0.1% gelatin-coated plates up to the fifth passage. GRK2 expression was monitored in MLECs from different genotypes by Western blot. Primary vascular smooth muscle (VSMC) cells were isolated from the aortas of GRK2+/+ and GRK2+/- mice as previously described (Mahabeleshwar et al.,

2006). MCF7, Hs578T, RAW267.4 and B16F10 cells (American Type Culture Collection) were maintained in Dulbecco's modified Eagle's medium (DMEM) supplemented with 10% (v/v) fetal bovine serum (FBS, Sigma-Aldrich), at 37ºC in a humidified 5% CO2 atmosphere. 184B5 cells were cultured in DMEM/F12-HAMS medium containing 5% horse serum, 10µg/ml insulin, 20ng/ml EGF, 100ng/ml cholera toxin, 0.5µg/ml hydrocortisone. For co-culture assays, different transformed (B16F10, MCF7 and Hs578T) and non-transformed (184B5) cell lines were seeded onto the bottom chamber of 12-well plates for 24h, while endothelial cells (MLEC) were plated onto gelatin-coated 24 mm Transwell inserts with 3.0-µm membrane pores (Costar) at a density of $6x10^4$ cells in the presence of culture medium in the upper chamber. When MLEC cells formed a monolayer, cells were serum-starved for 2h in DMEM plus Ham's F-12 medium supplemented with 1% FBS. Inserts were then placed in 12-well plates harboring confluent "bottom-plated" transformed and non-transformed cells and exposed to their influence for different times.

Cell Proliferation

DNA synthesis rates were determined by [^{3}H]thymidine uptake analysis. GRK2+/+ and GRK2+/- MLEC cells were seeded at 70% confluence in 24-well culture plates, serum-starved for 48h and then incubated with different mitogenic stimuli (1µM S1P, 20ng/ml VEGF or 5% fetal calf serum) for 24h. Cells were then pulse-labeled with 1µCi/ml [^{3}H]thymidine for the last 4h of stimulation, washed twice with PBS and incubated in 10% trichloroacetic acid at 4 °C for 10 min. DNA was solubilized in 0.2 M NaOH, 0.1% SDS for 2h at 37 °C. Radioactivity incorporated into DNA was determined in a scintillation β-counter.

Cell migration assays.

Primary aortic vascular smooth muscle (VSMC), the macrophage RAW267.4 cell line and MLEC cells isolated from GRK2 +/+ or GRK2+/- mice were serum-starved in 0.1% FBS or 0.5% FBS during 18h (for RAW267.4), and then seeded at a density of 60,000 VSMC cells/well, 30,000 MLEC cells/well or 100,000 RAW267.4 cells/well onto uncoated (for VSMC and RAW267.4) or gelatin (for MLEC)-coated 6.5-mm Transwell filters with 8-µm pores (Costar). Chemotaxis of VSMC and MLEC were assessed in the presence or absence of S1P (1µM), VEGF (20ng/ml) or PDGF-BB (50ng/ml). For migration experiments performed with RAW267.4 cells, 48-hour-conditioned media of MLEC isolated from wt GRK2 +/+ or TieCre-GRK2 f/f were used as the chemoattractant stimuli. Fibronectin (20 µg/ml)-coated filters were used to examine the integrin-mediated migration of MLEC. Cell treatment with the PI3K inhibitor LY294002 (10µM) was initiated 30 min before the migration assay and maintained thereafter by its addition to the upper cell chamber. After approx. 16h (VSMC and RAW267.4) or 5h (MLEC) of migration, cells were fixed, stained with DAPI 5µg/ml and counted in five random fields of each filter.

In vitro Tube Formation Assay on Matrigel and Image Analysis

MLEC cells were serum-starved for 3h and seeded onto 24-well culture plates coated with Matrigel (100µl/well). The cells were plated at a density of 1×10^5 cells/well in DMEM plus Ham's F-12 (1:1) supplemented with 1% FBS, and treated or not with S1P, TGFβ or FGF2 at the concentrations indicated for 16–18 h. Tube formation was observed with an Olympus IX51 inverted microscope and images were captured at 5x magnification with a CCD camera. For the evaluation of vessel-like formation, a set of 20-40 images for each experimental condition was analyzed using the web-based Image Analysis WinTube module of Wimasis. This online software tool allows the determination of parameters as branching points, tube length and number with statistics,

cell-covered area, net continuity and confluent area that reflects cellular growth in monolayers with less potential of tube formation. Tubular networks were described by the tube formation index (TF index), a function that integrate different aspects contributing either positively (the ratio of branching points to the total tubular skeleton or the tube mean length) or negatively (the ratio of confluent areas to the total cellular-covered area) to network extent and complexity. TF index= [mean tube length (px)]^2 x (total branching points/total tube length) X 1- [total confluent area (px)/covered cell area (px)].

Matrigel plug Assay for Angiogenesis in vivo.

Male and female 8-week-old mice of different GRK2 genotypes [systemic wild-type (GRK2+/+) and hemizygous (GRK2 +/-) animals or endothelium-specific modified Tie2Cre-GRK2 f/+, Tie2Cre-GRK2 f/- or Tie2Cre-GRK2 f/f individuals] were injected subcutaneously in the ventral region of the flank with 0.5 ml of Matrigel combined or not with FGF2 (0.5 µg/ml), S1P (5 µM) or VEGF (50ng/ml). Each Matrigel plug was harvested on day 7 and divided into two blocks, one being processed for hemoglobin determination with the TMB liquid substrate system according to the manufacturer's protocol, and another frozen in O.C.T compound (Tissue-Tek) for assessing formation of capillary-like structures by immunohistochemistry.

In vivo Tumor Implantation and Characterization of Tumor Angiogenesis

B16-F10 melanoma cells (1 x 10^6) in 100 µl of PBS supplemented with 0.1% glucose were subcutaneously implanted on the back of 8-week-old male and female mice [systemic wild-type (GRK2+/+ and GRK2 f/f) or hemizygous (GRK2 +/-) animals or endothelium-specific modified Tie2Cre-GRK2 f/- individuals]. The effects of macrophages on the differential growth of tumors implanted in endothelium- modified

GRK2 mice were assessed in two ways by using wild-type and Tie2Cre-GRK2 f/f animals. First, B16-F10 melanoma cells ($5x10^6$) were co-injected with or without M2-polarized RAW267.4 cells ($1x10^6$). Differentiation into the M2 phenotype was induced by overnight incubation of RAW267.4 cells with IL-4 (30U/ml). Second, B16-F10 melanoma cells ($5x10^6$) were implanted in wild-type (GRK2 f/f) or Tie2Cre-GRK2 f/f animals treated with either clodronate-encapsulated liposomes (Clodrosome, Encapsula NanoSciences LLC) or control liposomes (Encapsome) in order to induce in vivo depletion of murine macrophages. The mice (5-8/group) received an initial dose of Clodrosome or Encapsome (2mg/20g body weight in PBS) intraperitoneally administrated 1day before tumor cell implantation, followed by 1mg for the subsequent doses, injected every 3-4 days. To assess the efficacy of clodronate challenge on macrophage viability, thioglycolate-activated monocytes/macrophages were isolated from GRK2 f/f mice treated with Condrosome or Encapsome for 2-weeks by peritoneal lavage 3 days after intraperitoneal injection of 1 mL 3% sterile thioglycolate medium. Peritoneal monocyte numbers were drastically reduced in clodronate-treated [2,500 cells/ml (mice #1) and 87,000 cells/ml (mice #2)] compared to liposome control-treated animals [692,000 cells/ml (mice #3) and 915,000 cell/ml (mice #4)].

Tumor growth was monitored every day (RAW267.4 co-injected group) or once every three days with calipers. Tumor size was calculated as $(a)^2$ x b X 0,5236 (mm^3), where *a* and *b* represent the shortest and longest diameter of the tumor. When tumor volume exceeded the 10% of the total weight of the animal (over 2,000 mm3), mice were sacrificed for ethical reasons. For detection of tumoural hypoxia, pimonidazole (Hypoxiprobe TM-1 Plus kit, Hypoxiprobe, Inc) was injected intraperitoneally (2mg/100µl of 0.9% saline per mice) into wild-type (GRK2 +/+) or Tie2Cre-GRK2 f/f animals 60 min. before tumor mass removal. Tumors were processed for histological

analysis to analyze vascular structures. Tumor mass was excised and fixed with 3.7% paraformaldehyde (PFA)/PBS. Paraffin-embedded serial sections (3µm thickness) were dewaxed with xylene and rehydrated, followed by blocking of non-specific binding and endogenous peroxidase activity with 5% normal horse serum and 3% H_2O_2 solution, respectively. Slides were stained with biotinylated Lectin I Isolectin B4 (ILB4, 1:200) and α-SMA monoclonal antibody (1:1000) to detect endothelial and pericyte/vascular smooth muscle cells, respectively. Sections were then overlaid with secondary biotinylated goat anti-mouse IgG, followed by incubation with streptavidin-peroxidase conjugate. For chromogenic localization of antibodies, 3,3'-diaminobenzidine (DAB) was used. After optimal color development, sections were counterstained with Gill 2 hematoxylin (Thermo Scientific). Two different tumor specimens were analyzed per condition, and capillary diameter were quantified in 100-50 pictures taken on sections covering the entire tumor sample. For vessel size quantification, the area (µm) of ILB4-positive profiles (in an average of 600 and 400 for GRK2+/+ and Tie2Cre-GRK2 f/- tumors, respectively) was determined and the diameter calculated. Vessel size was ranked according to their diameter as follows: large (>70µm), medium (30-70µm) and small (<30µm). For determination of vessel pericyte coverage, tumor sections were double-stained with anti-mouse α-SMA (1:1000) and fluorescein-conjugated Isolectin B4 (1:150) to label mural and endothelial cells, respectively. Slides were then incubated with the secondary donkey anti-mouse IgG Alexa Fluor 555-conjugated antibody (Invitrogen) and sections were mounted on Mowiol. Positive signals were photographed under a fluorescent microscope coupled to a CDD camera (x40 objective magnification, Axiovert-200 Zeiss). The extent of pericyte coverage was calculated using the ImageJ software by calculating the proportion of α-SMA-stained area that overlaps with the ILB4-positive area.

For measurement of macrophage infiltration, antigen retrieval with proteinase K was performed and tumor sections were stained with the monoclonal antibody F4/80 (1:250). Samples were examined under an inverted microscope (Axiovert-200) and the number of macrophages per microscopic field (10X magnification) was recorded. At least 40 different fields were examined for each tumor specimen.

Embryo Characterization by Immunostaining

Embryos at 10.5 and 11.5 days post coitus (E10.5 and E11.5) were isolated and fixed in Dent's solution (80% methanol:20% DMSO). Dissected yolk sacs were examined under a stereoscopic microscopy with a coupled CCD camera, photographed and then subjected to genomic DNA extraction for genotyping. Fixed embryos were processed for cryosectioning and either to histological or immunofluorescence immunostaining. Sections were probed with different polyclonal anti-GRK2 (FP2 and C-15), anti-PECAM, anti-SMA, anti-laminin or anti-activated caspase-3 antibodies. Embryo samples were counterstained with hematoxylin and eosin according to the standard methods.

Vascular characterization of whole-mount retinas

Eyes from 9- and 14-days old GRK2 f/f and Tie2Cre-GRK2 f/f pups were enucleated and fixed in 2% PFA for 2h at room temperature, followed by two additional hours at 4 ^{o}C. Retinas were excised, washed in PBS plus 0.1% Igepal and permeabilized in 0.3% Triton/PBS for 2h. After incubation in blocking buffer (2% goat serum in PBS plus 0.1% Igepal) for 2h, retinas were washed with PBS plus 0.1% Igepal and PBS-lec (0.3% Triton, 0.1% goat serum, 0.1mM $CaCl_2$, 0.1mM MgCl2, 0.1mM MnCl2 in PBS). Then, retinas were incubated overnight at 4^{o}C with anti-NG2 antibody and FICT-ILB4 in PBS-lec. After extensive washing with PBS plus 0.1% Igepal, retinas were incubated

overnight at 4ºC with secondary anti-rabbit IgG Alexa Fluor 594-conjugated antibody diluted in washing buffer. Retinal flat mounts were then prepared in Mowiol. Images of whole mount retinas were acquired on a confocal microscope Zeiss LSM510 Meta. Image processing and measurement steps were performed using the software for image analysis ImageJ. To measure vascular (endothelial or perycite) densities, images were changed to gray scale and positive-stained area measured using the ImageJ´s thresholding tool and plotted as area fraction of total field area. For perycite coverage, area fraction of co-localizing pixels from pericyte- and endothelial-positive images was calculated. The number of branch points per field (10x amplification) and of filopodial extensions per field (63x amplification) was counted manually. Quantifications were performed on 11 retinas of P14 Tie2Cre-GRK2 f/f mice (n= 6), 8 retinas of P14 GRK2 f/f mice (n= 5), 18 retinas of P9 Tie2Cre-GRK2 f/f mice (n= 9) and 8 retinas of P9 GRK2 f/f mice (n= 5).

Immunohistochemistry analysis of Matrigel plugs and human breast tumors.

Frozen Matrigel plugs were sectioned at 8-µm thickness in a cryostat, and then fixed in acetone at -20°C for 15 minutes, followed by incubation of re-hydrated sections with 3% H_2O_2 solution for 10 min. Fixed sections were blocked by incubation with 5% normal horse serum and reacted overnight at 4ºC with rat monoclonal anti-CD31 (PECAM,1:20) or rabbit polyclonal antibody anti-NG2 (1:200). Sections were then stained with secondary biotinylated goat anti-rat or anti-rabbit IgG (Jackson ImmunoResearch Laboratories), followed by incubation with an avidin-biotin-peroxidase conjugate (Elite ABC kit) and DAB. Sections were hematoxylin-counterstained and images were recorded using an Olympus IX51 inverted microscope equipped with a CCD camera under X10 objective magnification. CD31 and NG2

quantification was performed by acquiring the area of positively stained pixels relative to the total Matrigel area from 5 random fields per condition with ImageJ software.

Human breast tissue samples from tissue array collections (Progression TMA breast carcinoma catalog CC08-00, Biomax, Cybrdi) and from patients treated at the Hospital Universitario La Paz (Madrid, Spain) were also analyzed by immunohistochemistry. 4-μm sections of paraffin-embedded tissues were deparaffinised and rehydrated in water, after which antigen retrieval was carried out by incubation in EDTA solution, pH 8.2 at 50ºC for 45 minutes. Endogenous peroxidase and non-specific antibody reactivity was blocked with peroxidase blocking reagent (Dako) at room temperature for 15 minutes. The sections were then incubated for 60-90 minutes at 4ºC with the anti-GRK2 PF2 polyclonal antibody. Detection was performed with Envision Plus Detection System (Dako). Negative controls were used with goat serum replacing the primary antibody. The slides were counterstained with haematoxylin and after drying were mounted with DPX mountant for microscopy (VWR Int).

Western blot Analysis.

To obtain total cell lysates, cells were washed with ice-cold PBS-buffer and subsequently solubilized in lysis buffer A (50mM Tris-HCl pH 7.5, 300mM NaCl, 1% Triton-X100, 0.1% SDS, 0.5% sodium deoxycholate and 1mM NaF, supplemented with 1 mM sodium orthovanadate plus a mixture of protease inhibitors). For embryo protein extraction, embryonic tissues were mechanically disrupted with liquid nitrogen and then lysed in buffer A. Cellular and embryonic lysates were resolved by 8-10% SDS-PAGE and immunoblotted with the indicated antibodies. ERK, AKT and Smad activation were determined and quantified by using their respective phospho-specific antibodies. Blots were then stripped and re-incubated with the respective antibodies to determine total amount of these proteins. Blots were developed using the chemiluminescence method

(ECL, Amersham Pharmacia Biotech). Bands were quantified by laser-scanner densitometry and Phospho-specific band densities were normalized to cognate total protein densities.

Analysis of **GRK2 mRNA Expression.**

Expression profiling by Serial Analysis of Gene Expression (SAGE) belonging to the Cancer Genome Anatomy Project SAGE library collection (CGAP: http://cgap.nci.nih.gov) was obtained from the GEO website using the identifier GSE15311. Vascular endothelium from normal or regenerating liver at different time points were isolated and processed to obtain SAGE libraries as described (Seaman et al., 2007). Numbers of total tags from the individual libraries corresponding to GRK2 probes were extracted.

Expression profiling using mouse Affymetrix microarrays of HMVECs co-cultured with tumor LS180 cells was previously described (Laubli et al., 2009). Raw data were downloaded from GEO website under the identifier GSE18113. GRK2 expression values in log2 scale was extracted from biological triplicates corresponding to quiescent HMVECs, HMVECs + blood components and HMVECs + blood components + LS180 human cancer colorectal pro-metastatic cell lines. Student's T-test was used to detect significant differences of gene expression.

Quantitative Analysis of PDGF-BB Secretion

PDGF-BB secretion by primary endothelial cells was determined by using a quantitative, solid-phase sandwich enzyme immunoassay technique to detect PDGF-BB (Quantikine mouse/rat PDGF-BB Immnunoassay, R&D Systems) following the manufacturer's instructions. MLEC cells isolated from GRK2+/+, GRK2+/- or GRK2+/+; Tie2Cre-GRK2$^{f/f}$ mice were plated in p60 dishes and allowed to grow at

confluence. The cells were then serum-starved for 24h in DMEM plus Ham's F-12 supplemented with 1%FCS, and incubated in the presence or absence of TGFβ (5ng/ml) or VEGF (20ng/ml) for the indicated times. Cell-conditioned media was harvested and concentrated 10-fold by lyophilization and the presence of PDGF-BB measured in duplicate and normalized to the total protein of conditioned media quantified by the Lowry method.

Analysis of Angiogenic Cytokine Profile of Primary Endothelial Cells

MLEC-GRK2+/+ and GRK2+/- cells ($7.5x10^5$ cells) were plated in p100 dishes and allowed to grow at confluence. After 48h of serum-starvation in DMEM plus Ham's F-12 supplemented with 1%FCS, cell-conditioned media were collected and concentrated by lyophilization to be analyzed by an enzyme-linked immunosorbent assay for a panel of molecules known to affect angiogenesis using the Mouse Angiogenesis Antibody Array I (RayBiotech) and the Mouse Angiogenesis Array Kit (R&D Systems) according to the manufacturer's protocol. Spot densities were quantitated by laser densitometric analysis and only signals of cytokine and angiogenic factors with values above 15% of the internal positive control were considered.

Vascular Permeability assay in vitro

MLEC cells isolated from GRK2+/+ or GRK2+/- mice were seeded on gelatin-coated transwells with 3μm pore size (Costar) at a density of 6×10^4 cells/cm^2 and allowed to form a monolayer. Permeability was stimulated with VEGF (20ng/ml) for 30 min followed by addition of HRP (1.5μg/ml) into the top chamber for additional 30 min. HRP activity was determined in the bottom chamber by a colorimetric method that detects increased absorbance at 490 nm caused by generation of the *O*-phenylenediamine reaction product (Stockton et al., 2004).

Supplemental Information References

Adini A, Kornaga T, Firoozbakht F, Benjamin LE. 2002. Placental growth factor is a survival factor for tumor endothelial cells and macrophages. *Cancer Res*. **6**:2749-52.

Belperio JA, Keane MP, Arenberg DA, Addison CL, Ehlert JE, Burdick MD, Strieter RM. 2000. CXC chemokines in angiogenesis. *J Leukoc Biol.* **68**:1-8.

Bornstein, P. 2009. Thrombospondins function as regulators of angiogenesis. *J Cell Commun Signal* 3:189-200.

Dirkx AE, Oude Egbrink MG, Wagstaff J, Griffioen AW. 2006 Monocyte/macrophage infiltration in tumors: modulators of angiogenesis. *J Leukoc Biol.* **80**:1183-96.

Gil-Bernabé AM, Ferjancic S, Tlalka M, Zhao L, Allen PD, Im JH, Watson K, Hill SA, Amirkhosravi A, Francis JL, Pollard JW, Ruf W, Muschel RJ. 2012. Recruitment of monocytes/macrophages by tissue factor-mediated coagulation is essential for metastatic cell survival and premetastatic niche establishment in mice. *Blood.* **119**:3164-75.

Jaber M, Koch WJ, Rockman H, Smith B, Bond RA, Sulik KK*, et al.* Essential role of beta-adrenergic receptor kinase 1 in cardiac development and function. *Proc Natl Acad Sci U S A* 1996,**93**:12974-12979.

Kiefer F, Siekmann AF. The role of chemokines and their receptors in angiogenesis. *Cell Mol Life Sci* 2011,**68**:2811-2830.

Laubli H, Spanaus KS, Borsig L. Selectin-mediated activation of endothelial cells induces expression of CCL5 and promotes metastasis through recruitment of monocytes. *Blood* 2009,**114**:4583-4591

Mahabeleshwar, G.H., Somanath, P.R., and Byzova, T.V. 2006. Methods for isolation of endothelial and smooth muscle cells and in vitro proliferation assays. *Methods Mol Med* 129:197-208.

Matkovich SJ, Diwan A, Klanke JL, Hammer DJ, Marreez Y, Odley AM*, et al.* Cardiac-specific ablation of G-protein receptor kinase 2 redefines its roles in heart development and beta-adrenergic signaling. *Circ Res* 2006,**99**:996-1003.

Penela P, Ribas C, Aymerich I, Eijkelkamp N, Barreiro O, Heijnen CJ*, et al.* G protein-coupled receptor kinase 2 positively regulates epithelial cell migration. *EMBO J* 2008,**27**:1206-1218.

Reynolds, L.E., Wyder, L., Lively, J.C., Taverna, D., Robinson, S.D., Huang, X., Sheppard, D., Hynes, R.O., and Hodivala-Dilke, K.M. 2002. Enhanced pathological angiogenesis in mice lacking beta3 integrin or beta3 and beta5 integrins. *Nat Med* 8:27-34

Seaman S, Stevens J, Yang MY, Logsdon D, Graff-Cherry C, St Croix B. Genes that distinguish physiological and pathological angiogenesis. *Cancer Cell* 2007,**11**:539-554

Smith DF, Galkina E, Ley K, Huo Y. 2005 GRO family chemokines are specialized for monocyte arrest from flow. *Am J Physiol Heart Circ Physiol.* **289**:H1976-84

Stockton, R.A., Schaefer, E., and Schwartz, M.A. 2004. p21-activated kinase regulates endothelial permeability through modulation of contractility. *J Biol Chem* 279:46621-46630.

Traves SL, Smith SJ, Barnes PJ, Donnelly LE. 2004. Specific CXC but not CC chemokines cause elevated monocyte migration in COPD: a role for CXCR2. *J Leukoc Biol.* **76**:441-50

Zhang L, Ran L, Garcia GE, Wang XH, Han S, Du J, Mitch WE. 2009. Chemokine CXCL16 regulates neutrophil and macrophage infiltration into injured muscle, promoting muscle regeneration. *Am J Pathol*. **175**:2518-27

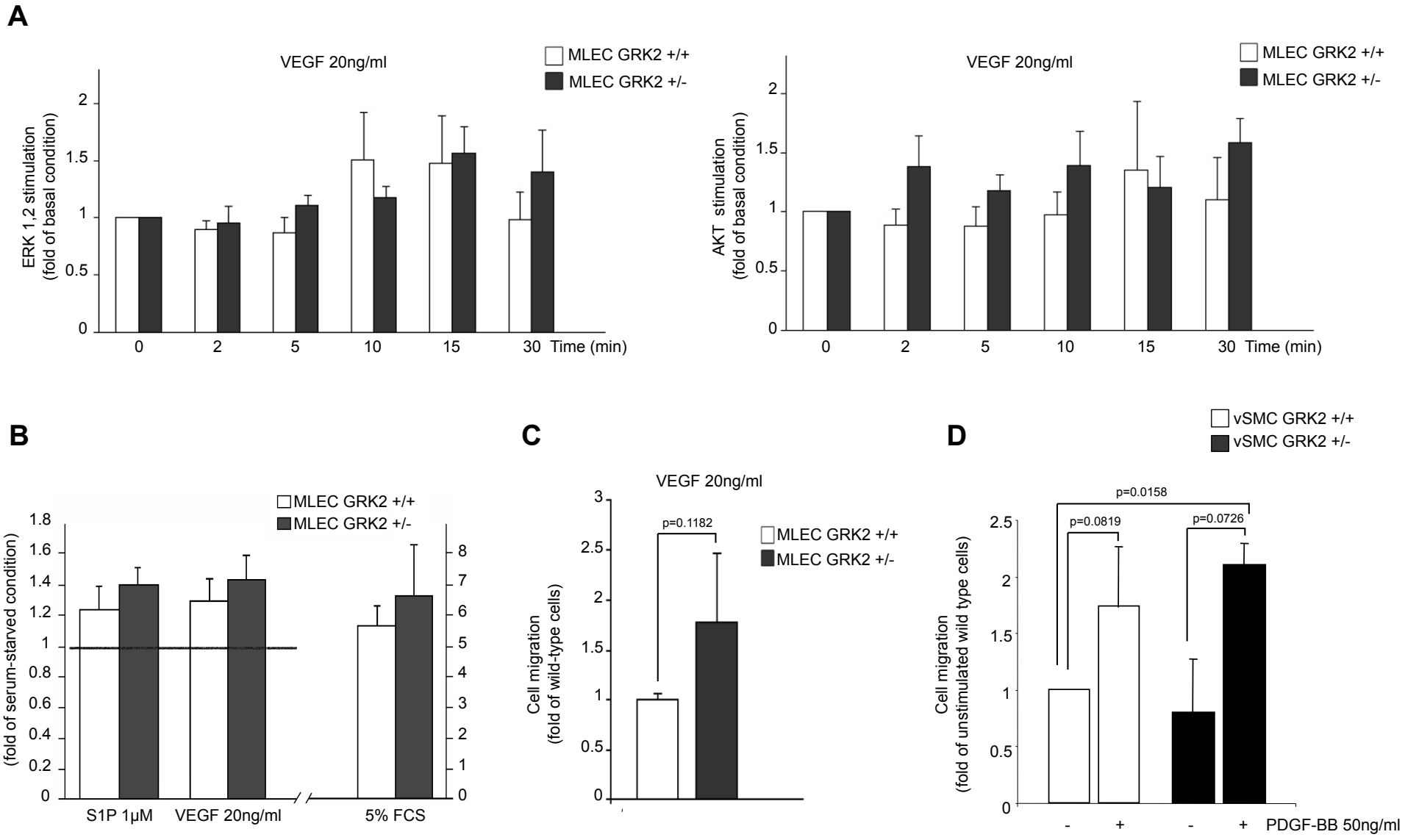
A
VEGF 20ng/ml
MLEC GRK2 +/+
MLEC GRK2 +/-
ERK 1,2 stimulation
(fold of basal condition)
0
0.5
1
1.5
2
0
2
5
10
15
30
Time (min)
VEGF 20ng/ml
MLEC GRK2 +/+
MLEC GRK2 +/-
AKT stimulation
(fold of basal condition)
0
0.5
1
1.5
2
0
2
5
10
15
30
Time (min)
B
MLEC GRK2 +/+
MLEC GRK2 +/-
Cell proliferation
(fold of serum-starved condition)
0
0.2
0.4
0.6
0.8
1
1.2
1.4
1.6
1.8
0
1
2
3
4
5
6
7
8
S1P 1µM
VEGF 20ng/ml
5% FCS
C
VEGF 20ng/ml
p=0.1182
MLEC GRK2 +/+
MLEC GRK2 +/-
Cell migration
(fold of wild-type cells)
0
0.5
1
1.5
2
2.5
3
D
vSMC GRK2 +/+
vSMC GRK2 +/-
p=0.0158
p=0.0819
p=0.0726
Cell migration
(fold of unstimulated wild type cells)
0
0.5
1
1.5
2
2.5
-
+
-
+
PDGF-BB 50ng/ml

Figure S1

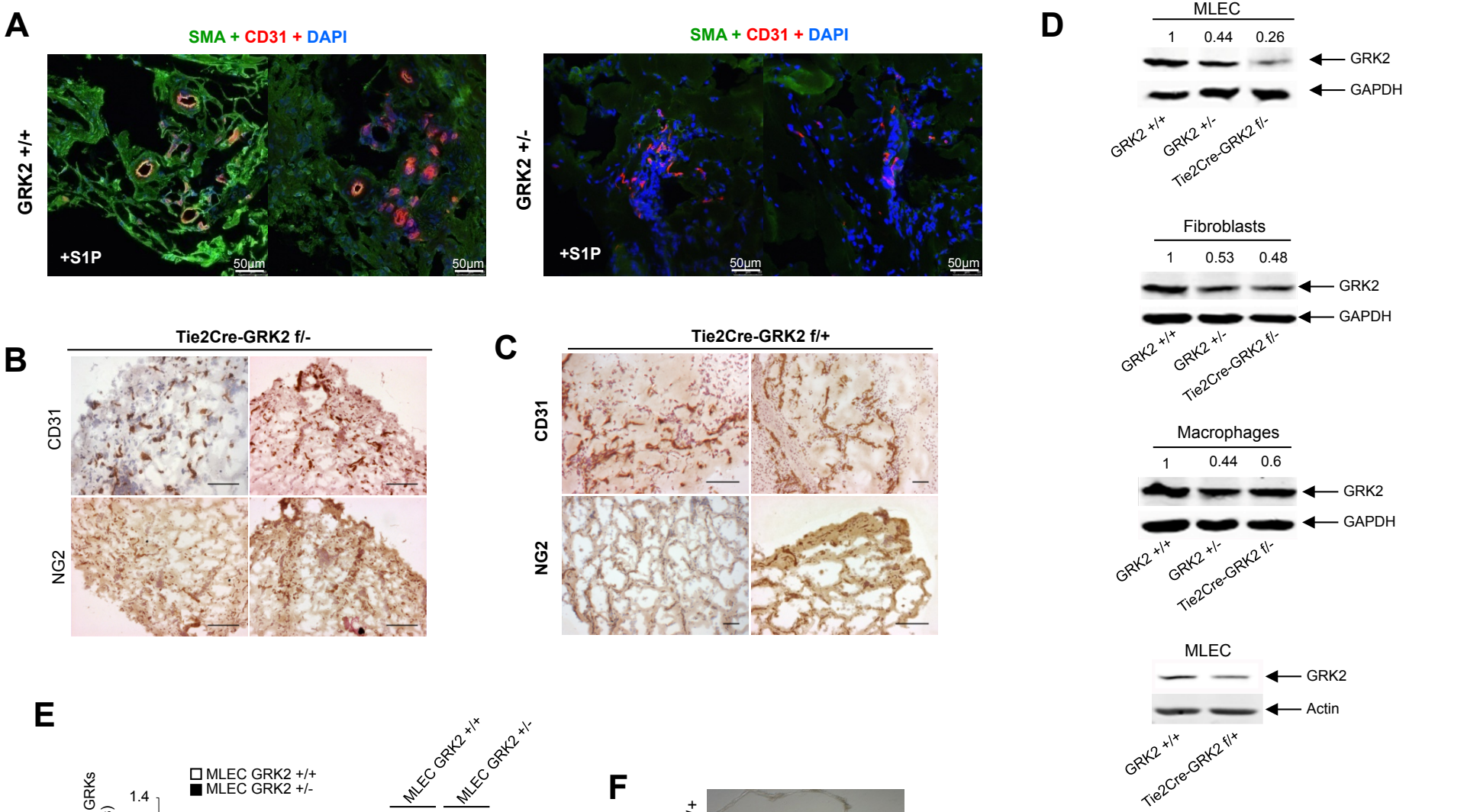
A
SMA + CD31 + DAPI
GRK2 +/+
+S1P
50µm
SMA + CD31 + DAPI
GRK2 +/-
+S1P
50µm
B
Tie2Cre-GRK2 f/-
CD31
NG2
C
Tie2Cre-GRK2 f/+
CD31
NG2
D
MLEC
1
0.44
0.26
GRK2
GAPDH
GRK2 +/+
GRK2 +/-
Tie2Cre-GRK2 f/-
Fibroblasts
1
0.53
0.48
GRK2
GAPDH
GRK2 +/+
GRK2 +/-
Tie2Cre-GRK2 f/-
Macrophages
1
0.44
0.6
GRK2
GAPDH
GRK2 +/+
GRK2 +/-
Tie2Cre-GRK2 f/-
MLEC
GRK2
Actin
GRK2 +/+
Tie2Cre-GRK2 f/+
E
MLEC GRK2 +/+
MLEC GRK2 +/-
Basal expression levels of GRKs (fold of wild-type cells)
1.4
1.2
1
0.8
0.6
0.4
0.2
0
GRK3
GRK6
MLEC GRK2 +/+
MLEC GRK2 +/-
GRK2
GRK3
actin
GRK6
actin
F
MLEC GRK2 +/+
MLEC GRK2 +/-
Tube Formation Index
70
60
50
40
30
20
10
0
p=0.0097
FGF2
MLEC GRK2 +/+
MLEC GRK2 +/-
Mean Tube length (pixels)
250
200
150
100
50
0
p=0.0276

Figure S2

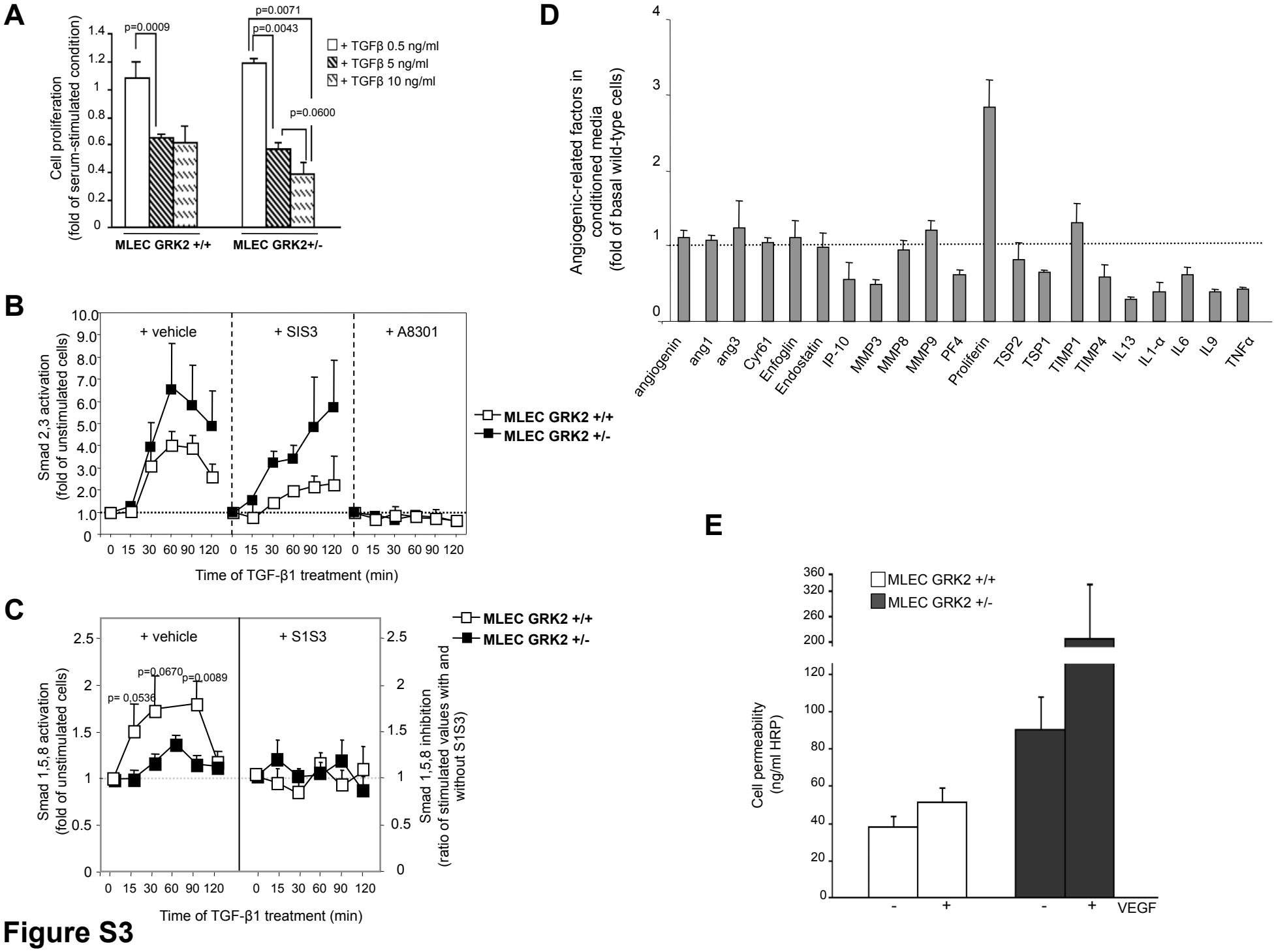
A
Cell proliferation
(fold of serum-stimulated condition)
p=0.0009
p=0.0071
p=0.0043
p=0.0600
+ TGFβ 0.5 ng/ml
+ TGFβ 5 ng/ml
+ TGFβ 10 ng/ml
MLEC GRK2 +/+
MLEC GRK2+/-
B
Smad 2,3 activation
(fold of unstimulated cells)
+ vehicle
+ SIS3
+ A8301
MLEC GRK2 +/+
MLEC GRK2 +/-
Time of TGF-β1 treatment (min)
C
Smad 1,5,8 activation
(fold of unstimulated cells)
+ vehicle
+ S1S3
p=0.0670
p=0.0089
p= 0.0536
Smad 1,5,8 inhibition
(ratio of stimulated values with and without S1S3)
MLEC GRK2 +/+
MLEC GRK2 +/-
Time of TGF-β1 treatment (min)
D
Angiogenic-related factors in conditioned media
(fold of basal wild-type cells)
angiogenin
ang1
ang3
Cyr61
Enfoglin
Endostatin
IP-10
MMP3
MMP8
MMP9
PF4
Proliferin
TSP2
TSP1
TIMP1
TIMP4
IL13
IL1-α
IL6
IL9
TNFα
E
MLEC GRK2 +/+
MLEC GRK2 +/-
Cell permeability
(ng/ml HRP)
VEGF

Figure S3

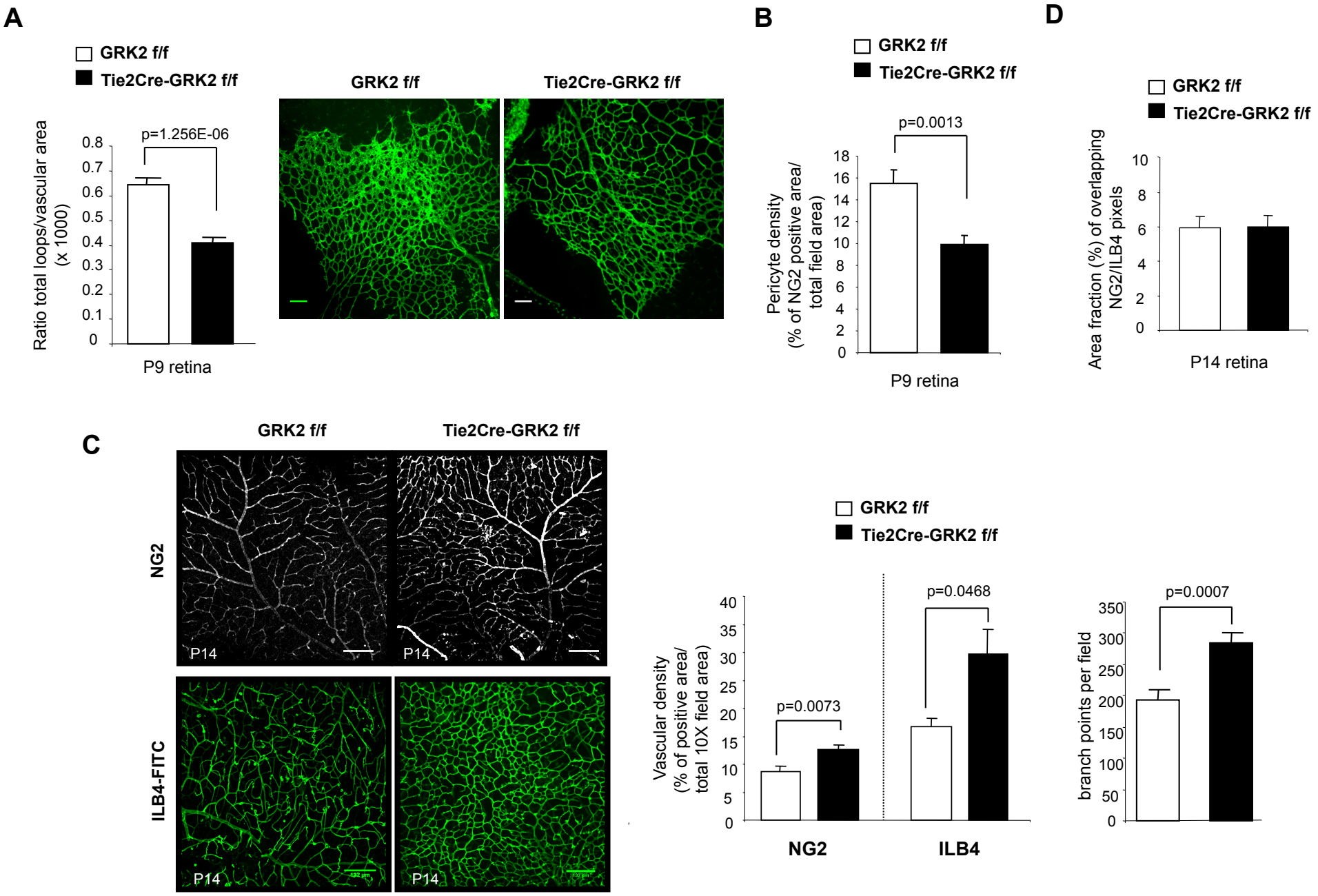
A
GRK2 f/f
Tie2Cre-GRK2 f/f
p=1.256E-06
Ratio total loops/vascular area (x 1000)
0.8
0.7
0.6
0.5
0.4
0.3
0.2
0.1
0
P9 retina
GRK2 f/f
Tie2Cre-GRK2 f/f
B
GRK2 f/f
Tie2Cre-GRK2 f/f
p=0.0013
Pericyte density (% of NG2 positive area/ total field area)
18
16
14
12
10
8
6
4
2
0
P9 retina
D
GRK2 f/f
Tie2Cre-GRK2 f/f
Area fraction (%) of overlapping NG2/ILB4 pixels
10
8
6
4
2
0
P14 retina
C
GRK2 f/f
Tie2Cre-GRK2 f/f
NG2
ILB4-FITC
P14
P14
P14
P14
GRK2 f/f
Tie2Cre-GRK2 f/f
p=0.0073
p=0.0468
Vascular density (% of positive area/ total 10X field area)
40
35
30
25
20
15
10
5
0
NG2
ILB4
p=0.0007
branch points per field
350
300
250
200
150
100
50
0

Figure S4

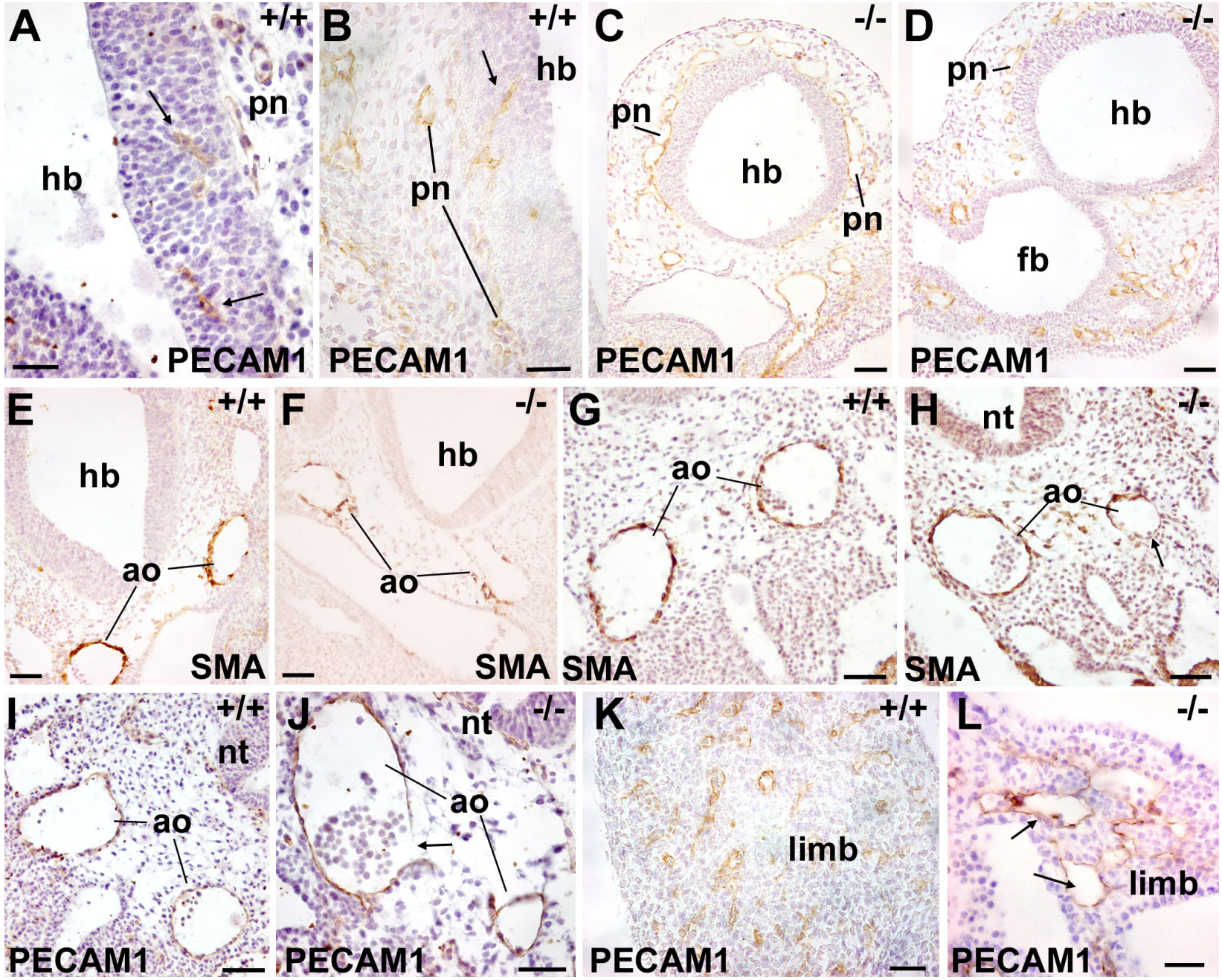
A
+/+
pn
hb
PECAM1
B
+/+
hb
pn
PECAM1
C
-/-
pn
hb
pn
PECAM1
D
-/-
pn
hb
fb
PECAM1
E
+/+
hb
ao
SMA
F
-/-
hb
ao
SMA
G
+/+
ao
SMA
H
nt
-/-
ao
SMA
I
+/+
nt
ao
PECAM1
J
nt
-/-
ao
PECAM1
K
+/+
limb
PECAM1
L
-/-
limb
PECAM1

Figure S5

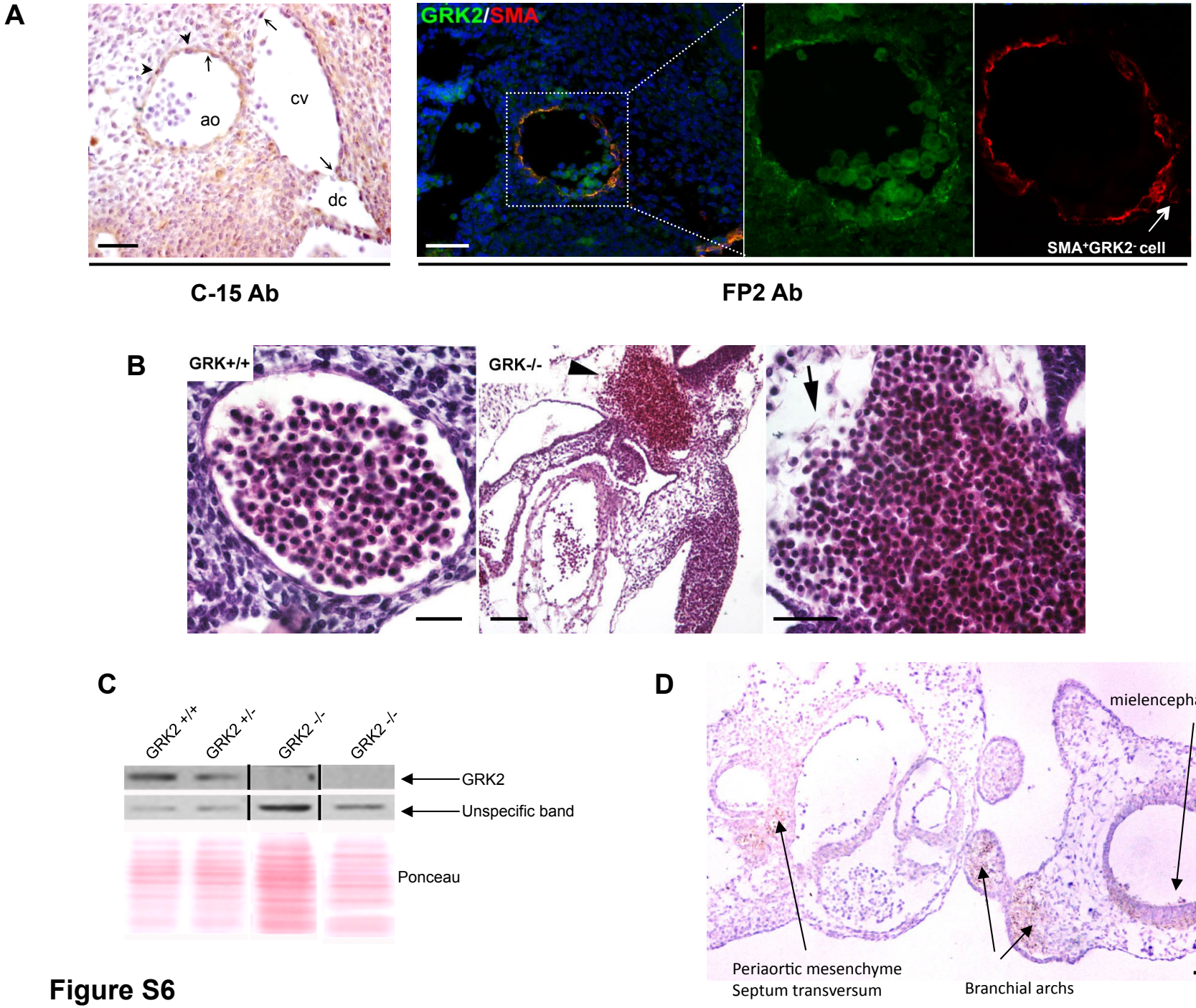
A
ao
cv
dc
GRK2/SMA
SMA+GRK2- cell
C-15 Ab
FP2 Ab
B
GRK+/+
GRK-/-
C
GRK2 +/+
GRK2 +/-
GRK2 -/-
GRK2 -/-
GRK2
Unspecific band
Ponceau
D
mielencephalon
Periaortic mesenchyme
Septum transversum
Branchial archs

Figure S6

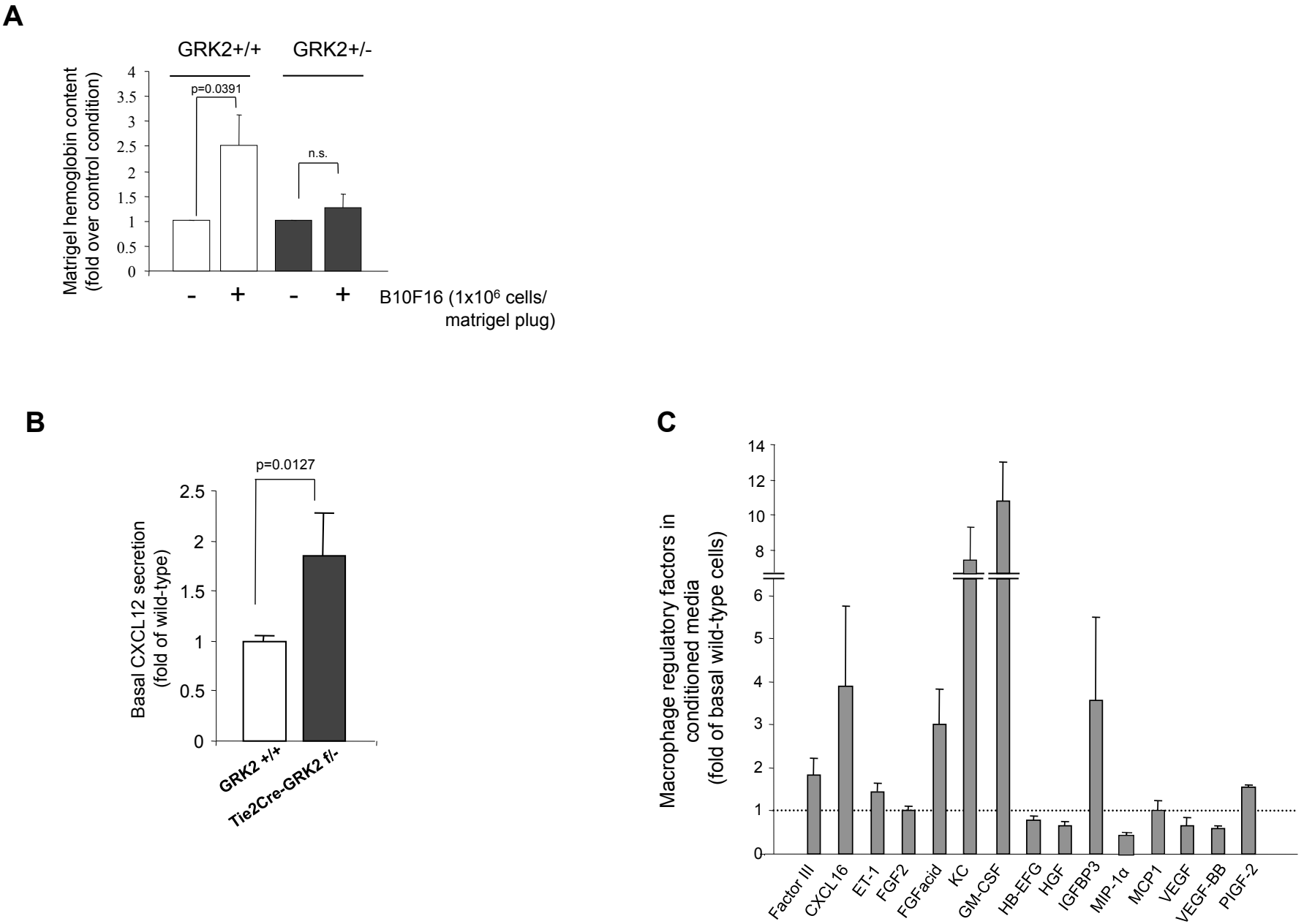
A
GRK2+/+
GRK2+/-
Matrigel hemoglobin content
(fold over control condition)
p=0.0391
n.s.
4
3.5
3
2.5
2
1.5
1
0.5
0
- + - +
B10F16 (1x10^6 cells/
matrigel plug)
B
p=0.0127
Basal CXCL12 secretion
(fold of wild-type)
2.5
2
1.5
1
0.5
0
GRK2 +/+
Tie2Cre-GRK2 f/-
C
Macrophage regulatory factors in
conditioned media
(fold of basal wild-type cells)
14
12
10
8
6
5
4
3
2
1
0
Factor III
CXCL16
ET-1
FGF2
FGFacid
KC
GM-CSF
HB-EFG
HGF
IGFBP3
MIP-1α
MCP1
VEGF
VEGF-BB
PIGF-2

Figure S7

A

GRK2 expression levels in regenerating mouse liver ECs.				
Normal Resting ECs	RL ECs			Gene Symbol
Liver	24 hr	48 hr	72 hr	
9	9	12	13	Grk2

B

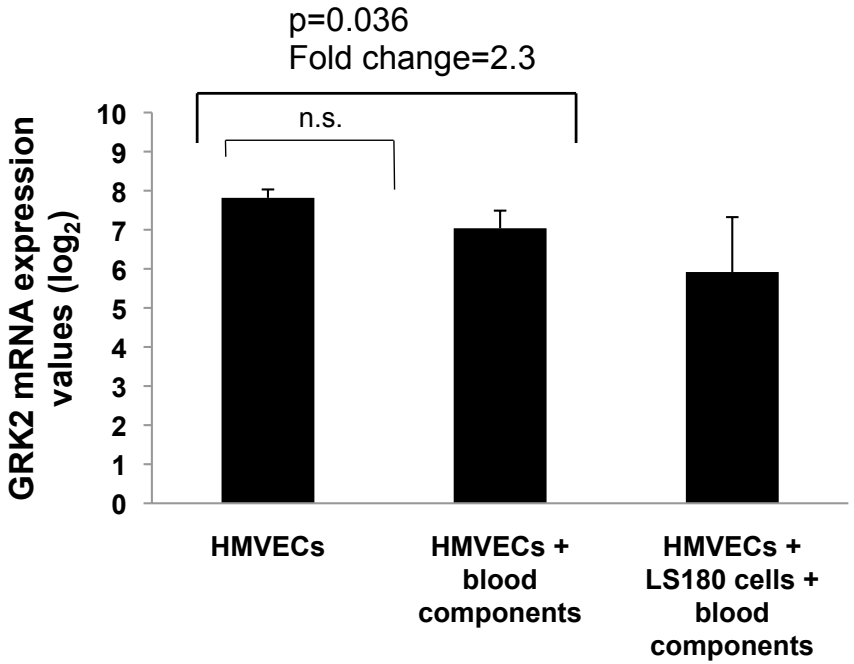

Figure S8